



HAL
open science

Well-controlled femtosecond laser inscription of periodic void structures in porous glass for photonic applications

Hongfeng Ma, Roman Zakoldaev, Anton Rudenko, Maksim M Sergeev, Vadim P Veiko, Tatiana Itina

► To cite this version:

Hongfeng Ma, Roman Zakoldaev, Anton Rudenko, Maksim M Sergeev, Vadim P Veiko, et al.. Well-controlled femtosecond laser inscription of periodic void structures in porous glass for photonic applications. *Optics Express*, 2017, 25 (26), 10.1364/OE.25.033261 . ujm-01671701

HAL Id: ujm-01671701

<https://ujm.hal.science/ujm-01671701>

Submitted on 22 Dec 2017

HAL is a multi-disciplinary open access archive for the deposit and dissemination of scientific research documents, whether they are published or not. The documents may come from teaching and research institutions in France or abroad, or from public or private research centers.

L'archive ouverte pluridisciplinaire **HAL**, est destinée au dépôt et à la diffusion de documents scientifiques de niveau recherche, publiés ou non, émanant des établissements d'enseignement et de recherche français ou étrangers, des laboratoires publics ou privés.

Well-controlled femtosecond laser inscription of periodic void structures in porous glass for photonic applications

HONGFENG MA,¹ ROMAN A. ZAKOLDAEV,² ANTON RUDENKO,¹
MAKSIM M. SERGEEV,² VADIM P. VEIKO,² AND TATIANA E. ITINA^{1,2,*}

¹Hubert Curien Laboratory, UMR CNRS 5516/UJM/University of Lyon, Bat. F, 18 rue du Pr. Benoit Laurus, 42000 Saint-Etienne, France

²ITMO University, 49 Kronverksky prospect, 197101 Saint Petersburg, Russia

*tatiana.itina@univ-st-etienne.fr

Abstract: We report control possibilities over ultrafast laser-induced periodic void lines in porous glass. Instead of high intensity regime leading to filaments, multi-pulse irradiation with high repetition rate (500 kHz) and various writing speed is used here in a transverse geometry. The formation of a perfectly controlled periodic void structure is shown to rely on such parameters as laser energy per pulse and scanning speed. In particular, both the threshold energy required for this effect and the period of the fabricated void arrays are shown to rise linearly with the number of the applied laser pulses per spot, or with a decreasing writing speed. To explain these results, a thermodynamic analysis is performed. The obtained dependencies are correlated with linear energy losses, whereas the periodicity of the observed structures is attributed to a static energy source formation at the void location affecting both material density and laser energy absorption.

© 2017 Optical Society of America under the terms of the [OSA Open Access Publishing Agreement](#)

OCIS codes: (140.7090) Ultrafast lasers; (160.2900) Optical storage materials; (350.3390) Laser materials processing.

References and links

1. R. Gattass and E. Mazur, "Femtosecond laser micromachining in transparent materials," *Nat. Photonics* **2**(4), 219–225 (2008).
2. R. Graf, A. Fernandez, M. Dubov, H. J. Brueckner, B. N. Chichkov, and A. Apolonski, "Pearl-chain waveguides written at megahertz repetition rate," *Appl. Phys. B: Lasers Opt.* **87**(1), 21–27 (2007).
3. Y. Bellouard and M.-O. Hongler, "Femtosecond-laser generation of self-organized bubble patterns in fused silica," *Opt. Express* **19**(7), 6807–6821 (2011).
4. C. Schaffer, A. Brodeur, and E. Mazur, "Laser-induced breakdown and damage in bulk transparent materials induced by tightly focused femtosecond laser pulses," *Meas. Sci. Technol.* **12**(11), 1784 (2001).
5. B. C. Stuart, M. D. Feit, A. M. Rubenchik, B. W. Shore, and M. D. Perry, "Laser-induced damage in dielectrics with nanosecond to subpicosecond pulses," *Phys. Rev. Lett.* **74**(12), 2248 (1995).
6. B. Rethfeld, "Free-electron generation in laser-irradiated dielectrics," *Phys. Rev. B* **73**(3), 035101 (2006).
7. R. Taylor, C. Hnatovsky, and E. Simova, "Applications of femtosecond laser induced self-organized planar nanocracks inside fused silica glass," *Laser Photonics Rev.* **2**(1-2), 26–46 (2008).
8. S. Richter, S. Döring, F. Burmeister, F. Zimmermann, A. Tünnermann, and S. Nolte, "Formation of periodic disruptions induced by heat accumulation of femtosecond laser pulses," *Opt. Express* **21**(13), 15452–15463 (2013).
9. N. Bulgakova, V. P. Zhukov, S. V. Sonina, and Y. P. Meshcheryakov, "Modification of transparent materials with ultrashort laser pulses: What is energetically and mechanically meaningful?" *J. Appl. Phys.* **118**(23), 233108 (2015).
10. N. Bloembergen, "A brief history of light breakdown," *J. Nonlinear Opt. Phys. Mater.* **6**(04), 377–385 (1997).
11. A. P. Joglekar, H.-H. Liu, E. Meyhöfer, G. Mourou, and A. J. Hunt, "Optics at critical intensity: Applications to nanomorphing," *PNAS* **101**(16), 5856–5861 (2004).
12. C. B. Schaffer, A. Brodeur, J. F. Garcia, and E. Mazur, "Micromachining bulk glass by use of femtosecond laser pulses with nanojoule energy," *Opt. Lett.* **26**(2), 93–95 (2001).
13. I. Miyamoto, K. Cvecek, and M. Schmidt, "Evaluation of nonlinear absorptivity in internal modification of bulk glass by ultrashort laser pulses," *Opt. Express* **19**(11), 10714–10727 (2011).
14. V. P. Veiko, E. A. Shakhno, and E. B. Yakovlev, "Effective time of thermal effect of ultrashort laser pulses on dielectrics," *Quantum Electron.* **44**(4), 322 (2014).
15. W. Watanabe, T. Toma, K. Yamada, J. Nishii, K. Hayashi, and K. Itoh, "Optical seizing and merging of voids in silica glass with infrared femtosecond laser pulses," *Opt. Lett.* **25**(22), 1669–1671 (2000).

16. S. Juodkazis, K. Nishimura, S. Tanaka, H. Misawa, E. G. Gamaly, B. Luther-Davies, L. Hallo, P. Nicolai, and V. T. Tikhonchuk, "Laser-induced microexplosion confined in the bulk of a sapphire crystal: evidence of multimegabar pressures," *Phys. Rev. Lett.* **96**(16), 166101 (2006).
17. M. Lancry, B. Pommellec, J. Canning, K. Cook, J.-C. Poulin, and F. Brisset, "Ultrafast nanoporous silica formation driven by femtosecond laser irradiation," *Laser Photonics Rev.* **7**(6), 953–962 (2013).
18. E. G. Gamaly, S. Juodkazis, K. Nishimura, H. Misawa, B. Luther-Davies, L. Hallo, P. Nicolai, and V. T. Tikhonchuk, "Laser-matter interaction in the bulk of a transparent solid: Confined microexplosion and void formation," *Phys. Rev. B* **73**(21), 214101 (2006).
19. L. Hallo, A. Bourgeade, V. T. Tikhonchuk, C. Mezel, and J. Breil, "Model and numerical simulations of the propagation and absorption of a short laser pulse in a transparent dielectric material: Blast-wave launch and cavity formation," *Phys. Rev. B* **76**(2), 024101 (2007).
20. C. Mézel, L. Hallo, A. Bourgeade, D. Hébert, V. T. Tikhonchuk, B. Chimier, B. Nkonga, G. Schurtz, and G. Travaillé, "Formation of nanocavities in dielectrics: A self-consistent modeling," *Phys. Rev. B* **15**(9), 093504 (2008).
21. L. Rapp, R. Meyer, R. Giust, L. Furfaro, M. Jacquot, P. A. Lacourt, J. M. Dudley, and F. Courvoisier, "High aspect ratio micro-explosions in the bulk of sapphire generated by femtosecond Bessel beams," *Sci. Rep.* **6**, 34286 (2016).
22. A. Rudenko, J.-P. Colombier, and T. E. Itina, "From random inhomogeneities to periodic nanostructures induced in bulk silica by ultrashort laser," *Phys. Rev. B* **93**(7), 075427 (2016).
23. A. Cerkauskaitė, R. Drevinskas, A. O. Rybaltovskii, and P. G. Kazansky, "Ultrafast laser-induced birefringence in various porosity silica glasses: from fused silica to aerogel," *Opt. Express* **25**(7), 8011–8021 (2017).
24. V. P. Veiko, S. I. Kudryashov, M. M. Sergeev, R. A. Zakoldaev, P. A. Danilov, A. A. Ionin, T. V. Antropova, and I. N. Anfimova, "Femtosecond laser-induced stress-free ultra-densification inside porous glass," *Laser Phys. Lett.* **13**(5), 055901 (2016).
25. S. Kanehira, J. Si, J. Qiu, K. Fujita, and K. Hirao, "Periodic nanovoid structures via femtosecond laser irradiation," *Nano Lett.* **5**(8), 1591–1595 (2005).
26. H. Sun, J. Song, C. Li, J. Xu, X. Wang, Y. Cheng, Z. Xu, J. Qiu, and T. Jia, "Standing electron plasma wave mechanism of void array formation inside glass by femtosecond laser irradiation," *Appl. Phys. A* **88**(2), 285–288 (2007).
27. J. Song, X. Wang, X. Hu, Y. Dai, J. Qiu, Y. Cheng, and Z. Xu, "Formation mechanism of self-organized voids in dielectrics induced by tightly focused femtosecond laser pulses," *Appl. Phys. Lett.* **92**(9), 092904 (2008).
28. X. Wang, F. Chen, Q. Yang, H. Liu, H. Bian, J. Si, and X. Hou, "Fabrication of quasi-periodic micro-voids in fused silica by single femtosecond laser pulse," *Appl. Phys. A* **102**(1), 39–44 (2011).
29. Md. S. Ahsan, Y.-Y. Kwon, I.-B. Sohn, Y.-C. Noh, and M. S. Lee, "Formation of periodic micro/nano-holes array in boro-aluminosilicate glass by single-pulse femtosecond laser machining," *J. Laser Micro/Nanoeng.* **9**(1), 19 (2014).
30. K. Cvecek, I. Miyamoto, and M. Schmidt, "Gas bubble formation in fused silica generated by ultra-short laser pulses," *Opt. Express* **22**(13), 15877–15893 (2014).
31. S. Matsuo and S. Hashimoto, "Spontaneous formation of 10- μ m-scale periodic patterns in transverse-scanning femtosecond laser processing," *Opt. Express* **23**(1), 165–171 (2015).
32. A. Wu, I. H. Chowdhury, and X. Xu, "Femtosecond laser absorption in fused silica: Numerical and experimental investigation," *Phys. Rev. B* **72**(8), 085128 (2005).
33. L. V. Keldysh, "Diagram technique for nonequilibrium processes," *Sov. Phys. JETP* **20**(4), 1018–1026 (1965).
34. A. Kaiser, B. Rethfeld, M. Vicanek and G. Simon, "Microscopic processes in dielectrics under irradiation by subpicosecond laser pulses," *Phys. Rev. B* **61**(17), 11437 (2000).
35. J. R. Gully, S. W. Winkler, W. M. Dennis, C. M. Liebig and R. Stoian, Razvan, "Interaction of ultrashort-laser pulses with induced undercritical plasmas in fused silica," *Phys. Rev. A* **85**(1), 013808 (2012).
36. D. E. Grady, "The spall strength of condensed matter," *J. Mech. Phys. Solids* **36**(3), 353–384 (1988).
37. V. M. Sura and P. C. Panda, "Viscosity of porous glasses," *J. Am. Ceram. Soc.* **73**(9), 2697–2701 (1990).
38. A. R. Boccacini, "Viscosity of porous glasses," *J. Mater. Sci.* **30**(22), 5663–5666 (1995).

1. Introduction

The capacity of femtosecond laser systems to locally modify transparent materials has been used for many promising applications in different areas ranging from photonics to microfluidics [1]. The main advantage of the ultra-short laser pulses is in an extremely high precision of the energy deposition. Therefore, laser machining can be performed in volume of different glasses enabling three-dimensional inscription of numerous structures, such as photonics crystals, optical memories, waveguides, gratings, couplers, chemical and biological membranes and other devices [2, 3]. Previous studies have already revealed major mechanisms of femtosecond laser irradiation of typical glasses, such as fused silica, BK7 and calcium fluoride [4–9]. Such phenomena as photoionization and avalanche ionization leading to laser-induced breakdown were in focus of both experimental and theoretical studies starting from the invention of high-power systems [4, 10]. It was shown that very small regions could be efficiently treated in a

well-determined way by using only a central part of the Gaussian radial distribution of the laser beam [11].

The results of laser machining can considerably differ if instead of a single laser pulse, trains of high repetition rate ultra-short laser pulses are used [12, 13]. In fact, when time between laser pulses is shorter than that required for energy diffusion outside laser-treated volume, a considerable heat accumulation may lead to a pronounced enhancement in the size of the laser-affected zone. This effect was observed in the experiments with nanojoule laser energy at laser repetition rate as high as 25MHz . For such multi-pulse laser irradiation regime Miyamoto et al. [13] calculated thermal fields revealing stationary regimes for several optical materials and laser parameters. Moreover, it was shown that even upon a single ultra-short laser interaction with glass, the induced thermal effects could last for a significant time up to nanoseconds in dielectric materials [14].

Additionally, femtosecond laser-induced formation of nanopores and voids was investigated for the initially non-porous optical materials [3, 15–17]. Such effects as strong explosion and shock wave formation were shown to play a role in a single void formation for tightly focusing conditions [9, 18–21], whereas cavitation and nanopores were found to play a role in volume leading to nanograting formation when laser focusing was not so strong [17, 22, 23].

It was demonstrated, furthermore, that silica glasses with different densities including fused silica, porous glass, and aerogel could be also successfully processed [23, 24]. For porous glasses, several regimes were identified [24] with different corresponding types of material modifications ranging from densification and microvoid formation to wider channels appearance. In fact, laser-induced densification is expected in the regime of lower energy deposition, whereas the formation of channels was reported for larger laser absorbed energy. For intermediate absorbed energy, the so-called "decompaction" regime was identified accompanying by microscopic void formation during transverse laser scanning of porous glass in volume. We note that local control of porosity also allows the formation of waveguides and other embedded elements. Additionally, porous materials can be used for laser-assisted nanoparticle formation with promising photonic, plasmonic or photochromic properties. These investigations also open up a way toward an easier fabrication of optical sensors based on porous materials to monitor changes in the environment.

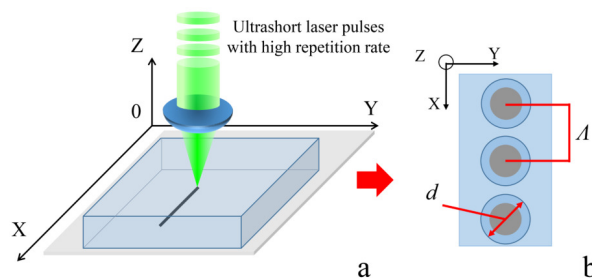


Fig. 1. Illustration of transverse laser scanning geometry (a) and the final structure (b).

Previously, ultra-short lasers were shown to induce voids both in the direction of laser propagation and in the laser scanning direction. The former structures were attributed to such effects as self-focusing and filamentation [25], standing electron plasma wave [26] or spherical aberration [27–29]. The transverse laser scanning of non-porous glass (Fig. 1) was performed only in a few studies and mostly for non-porous glasses [3, 8, 30, 31]. In particular, femtosecond-laser pulses were shown to generate self-organized bubble patterns [3] in fused silica at repetition rate as high as 9.4MHz and scanning speed up to 31mm/s . A transition between chaotic and self-organized patterns at high scanning rate (above 10mm/s) was revealed and attributed to similarities with rather complicated non-linear dynamical systems.

Thus, an efficient control over laser inscription is still puzzling, particularly for porous glasses. In fact, no systematized control possibilities over threshold, size or period have been proposed so far. That is why the present study is aimed at the identification of the major physical mechanisms involved in the ultra-short laser-induced void structure formation in volume of a porous glass. Such parameters as structure periodicity, size and the required pulse energy will be explained.

2. Results and discussion

2.1. Experiments

A series of experiments have been performed for porous silica glass plates. Their chemical composition is (mass fraction, %): 94.73SiO_2 - $4.97\text{B}_2\text{O}_3$ - $0.30\text{Na}_2\text{O}$ and the expected trace content (≤ 0.1 mass %) of Al_2O_3 . The average pore radius is $\approx 2\text{nm}$, the porosity $0.26\text{cm}^3/\text{cm}^3$, and the specific surface area of the pores is $\approx 210\text{m}^2/\text{g}$. The transmission of the used porous glass is high in the visible and near-IR range of wavelengths ($0.2 - 2.5\mu\text{m}$). The experimental set-up is shown in Fig. 2. Here, Satsuma Yb-doped fiber laser with wavelength $\lambda = 515\text{nm}$ at second-harmonic, temporal pulse width $\tau = 200\text{fs}$ passes through a nonlinear optical crystal (3) and a plate (4) placed at 45° angle to the laser beam direction (1). Material modifications are obtained by varying sample moving speed, V_s , from $0.0125 - 3.75\text{mm/s}$ with respect to the focused laser beam and by changing laser pulse energy E_p from 1.5 to $2.34\mu\text{J}$ at a constant repetition rate ($\nu = 500\text{kHz}$).

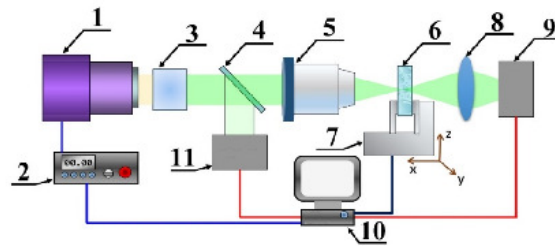


Fig. 2. Illustration of the experimental setup, where tightly focused ($20\times$, $NA = 0.4$) ultra-short laser pulses (200fs , 500kHz , 515nm) create decompaction region inside of the porous glass.

In this case, around 5 percents of laser energy is reflected from the plate (4) and arrives at the power measuring device (11). Then, the laser beam is focused by the objective (5) (LOMO, $20\times$, $NA = 0.4$) in volume of the glass film/plate (6) at the plane of the laser modified region formation (MR). When laser (1) is turned on, the optical table (7) (Standa 8SMC1-USBhF) starts moving along one of the axis X or Y. At the same time, a part of the transmitted laser radiation is registered by the power-meter (9) located behind the collective lens (8) placed right after the glass plate (6). Another part of the laser energy that is reflected by the place (4) is used to control laser power. The control over the optical table (7) movement and its synchronization with laser power supply (2) is provided by the personal computer (10).

At rather low laser energy and the number of laser shots per focusing spot, a moderate densification, or, compaction is observed in the porous glass. In the intermediate range of laser energy per pulse and of the number of laser pulses per spot, the decompaction structure is observed (Fig. 3) and is typically characterized by a series of voids with a size up to ten micrometers, which changes only slightly with the number of laser pulses per focusing spot. Importantly, the observed microvoids appear with a periodicity from a few microns to several tens of micrometers (Figs. 3 and 4(a)) in the considered laser irradiation regime. The distance between the voids can be varied by the total laser energy delivered per focusing diameter, E_p , or by the number of laser

pulses per spot, N , determined by the scanning speed. Here, a couple of interesting observations can be done.

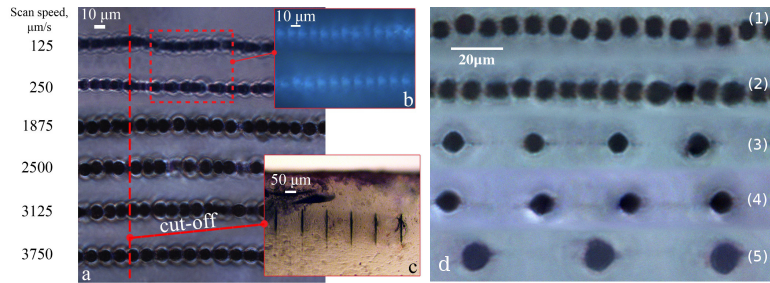


Fig. 3. (a-c) Optical transmission microscopy of decompaction regions obtained for different writing speeds; (d) image of periodic lines of voids formed inside of the porous glass at a constant pulse energy ($E_p = 2.2\mu J$) and with different number of pulses per focusing spot: (1) 2600, (2) 3200, (3) 5330, (4) 32000 and (5) 80000.

Firstly, the period $\Lambda \sim \xi N$, increases almost linearly with N (or, decreasing scanning speed), where ξ is a constant length defined by the slope of the line in Fig. 4(a). Here, $\xi \approx 0.62nm$. Secondly, the performed experiments clearly demonstrate that the laser energy required for the formation of the decompaction structures (energy threshold) also linearly increases with the number of the applied laser pulses per laser irradiated spot (Fig. 4(b)). Here, $E_a = E_0 \times N$, where E_0 depends on the focusing conditions and is on the order of $2.5\mu J$.

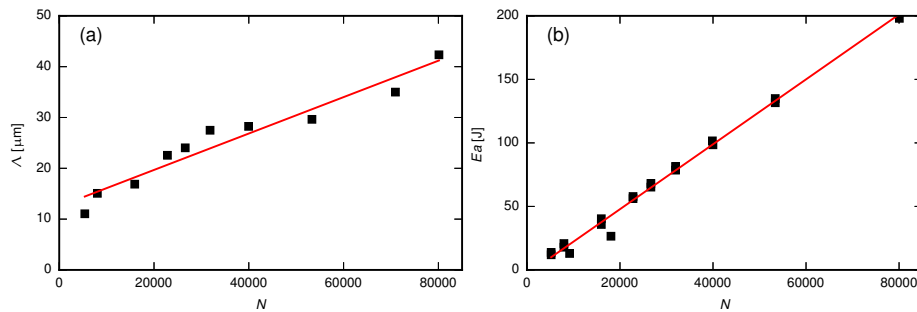


Fig. 4. (a) The period of the decompaction regions as a function of the number of laser pulses per spot at a constant pulse energy ($E_p = 2.2\mu J$); (b) the total threshold energy required to obtain the decompaction of PG using mentioned experimental setup as a function of the number of pulses per focusing spot.

2.2. Modeling and discussion

To explain the obtained experimental results, a thermodynamic analysis of the laser heating is performed. Every applied femtosecond laser pulses generates and heats free carries inside the glass. The subsequent electron-ion/matrix relaxation takes place on a picosecond time scale. In the considered multi-pulse regime, however, material temperature, or "base temperature" [13, 32] rises during longer time, t_h , corresponding to the focal spot irradiation time and creating an almost spherical region of the energy accumulation (Fig. 5(a)). This region can be then considered as a static heat source which appears consecutively in addition to the moving laser. Note, that the involved physical processes occur on very different time scales, where the energy relaxation stage is much longer than the laser absorption and heating ones.

The thermodynamic analysis is based on a modification of the procedure proposed by Miyamoto et al. [13, 26] for multi-pulse laser irradiation regime. In our model, both light propagation and energy absorption per shot are calculated by using nonlinear Schrödinger equation (NLSE) coupled with material ionization including photoionization, avalanche and electron trapping [32]. The effective optical index of the studied porous glass [24], n_0 , is estimated ≈ 1.342 according to the effective medium theory, e.g. Maxwell-Garnett theory. Moreover, the photoionization rate is calculated by using Keldysh theory [33]. The NLSE equation used here is written as follows

$$j \frac{\partial}{\partial z} \varphi = -\frac{1}{2k} \nabla_{\tau}^2 \varphi + \frac{v_g}{2} \frac{\partial^2 \varphi}{\partial t^2} - k \Delta n \varphi \quad (1)$$

where $\varphi(x, y, z, t)$, ∇_{τ} , k and $v_g \approx 361 \text{ fs}^2/\text{cm}$ are the envelop function of the electric field, the Laplacian operator in the XY plane, the wave number and the group velocity dispersion coefficient, respectively. The term Δn includes the optical index change and photoionization,

$$\Delta n = j \frac{W_{PI} U_g}{n \varepsilon_0 c_0 |\varphi|^2 k} + n_2 \frac{n \varepsilon_0 c_0 |\varphi|^2}{2} + j \frac{\sigma_B \rho}{2k} - \frac{\sigma_B \omega \tau_s \rho}{2k} \quad (2)$$

where W_{PI} is the photoionization rate and the related to material properties, such as band gap $U_g = 9 \text{ eV}$, electromagnetic wave angular frequency ω , effective mass of electron $m \approx 0.86 m_e$, and the light intensity [33]. $m_e \approx 9.1 \times 10^{-31} \text{ kg}$ is the free electron mass. The temporal optical index during pulsed laser, n , is estimated by Drude model, and $n_2 \approx 3.5 \times 10^{-16} \text{ cm}^2/\text{W}$, $\varepsilon_0 \approx 8.854 \times 10^{-12} \text{ F/m}$, $c_0 \approx 2.9979 \times 10^8 \text{ m/s}$, $\tau_s \approx 1.0 \text{ fs}$ are the Kerr-effect coefficient, vacuum permittivity, light speed in vacuum and electron collision time, respectively. σ_B is the cross section for inverse Bremsstrahlung absorption, $\sigma_B = (e^2 \tau_s / m (\omega^2 \tau_s^2 + 1) \cdot (1/n c_0 \varepsilon_0))$, where $e \approx 1.6022 \times 10^{-19} \text{ C}$ is the elementary charge. The free electron density is described by the following single rate equation during photoionization [32]

$$d\rho/dt = (W_{PI} + \eta I \rho)(1 - \rho/\rho_m) - \rho/\tau_p \quad (3)$$

which takes into account the multi-photon ionization, avalanche $\eta = \sigma/U_{eff}$ and electron relaxation time $\tau_p \approx 150 \text{ fs}$. Here, ω_0 , λ , $\rho_m \approx 2.2 \times 10^{22} \text{ cm}^{-3}$, $I = n c_0 \varepsilon_0 |\varphi|^2 / 2$ and $U_{eff} = (1 + m/m_e) \cdot (U_g + e^2 |\varphi|^2 / 4m\omega^2)$ [34] are the waist radius, maximum plasma density, laser wavelength in vacuum, laser intensity and effective band gap, respectively. The solution of these equations results in the following distribution of the total absorbed energy

$$q(z) = \pi \omega_0^2 \left[1 + \left(\frac{\lambda z}{\pi \omega_0^2 n_0} \right)^2 \right] \int_t \frac{4\pi \cdot \text{imag}(n)}{\lambda} I(z, t) dt \quad (4)$$

Finally, thermal behavior at time t is considered as a heating by consecutive laser sources separated along the scanning direction with distances of V_s/v . The analytical solution of the thermal equation is derived by Green's function method as follows [13]

$$\Delta T(x, y, z, t) = \frac{1}{\pi \rho_g c_g} \sum_{i=0}^N \frac{1}{\sqrt{\pi \alpha (t - i/v)}} Q_i \quad (5)$$

$$Q_i = \int \frac{q(z)}{\omega_z^2 + 8\alpha(t - i/v)} \exp\left[-\frac{2\{[x + V_s(t - i/v)]^2 + y^2\}}{\omega_z^2 + 8\alpha(t - i/v)} - \frac{(z - z')^2}{4\alpha t}\right] dz' \quad (6)$$

where $\omega_z = \omega_0 \sqrt{1 + \left(\frac{\lambda z}{\pi \omega_0^2 n_0} \right)^2}$ is the estimation of laser beam radius along z axis. Thermal parameters such as mass density ρ_g , heat capacity c_g and thermal diffusivity α are shown in Table 1. With all these equations at hand, we estimate the temperature distribution and evolution during

multi-pulse laser scanning. Fig. 5 shows the 2D base temperature distribution and evolution at various scanning speed.

The formation of the periodic patterns in multi-pulse regime is often attributed to the heat accumulation [2, 31]. In ultra-short laser processing, heat accumulation is typically considered as non-negligible when time between successive laser pulses, $\delta t = 1/\nu$, becomes shorter than the characteristic cooling time of the focal spot. When these times are comparable as in the present study (laser repetition rate is 500kHz), heat can escape from the focal region avoiding strong thermo-mechanical effects.

Table 1. Parameters summary used in simulation

Parameter	Description	Value or definition	Reference
λ	Laser wavelength in vacuum	515 nm	
n_0	Effective optical index of porous glass	1.342	
v_g	Group velocity dispersion coefficient	361 fs ² /cm	Ref([32, 35])
m_e	Free electron mass	9.1×10^{-31} kg	
m	Effective electron mass	$0.86m_e$	Ref([32])
n_2	Nonlinear refractive index	3.5×10^{-16} cm ² /W	Ref([32])
ϵ_0	Vacuum permittivity	9.954×10^{-12} F/m	
c_0	Light velocity	2.9979×10^8 m/s	
τ_s	Electron collision time	1.0 fs	Ref([32])
τ_p	Electron relaxation time	150 fs	Ref([32])
e	Elementary charge	1.6022×10^{-19} C	
ρ_m	Maximum plasma density	2.2×10^{22} cm ⁻³	Ref([32])
U_g	Material band gap	9 eV	
τ	Pulse duration	200 fs	
ν	Repetition rate	500 kHz	
V_s	Scanning speed	0.125 – 100 mm/s	
ω_0	Laser beam waist radius	2.45 – 2.6 μ m	
E_p	Pulse energy	1.5 – 2.3 μ J	
ρ_g	Mass density of porous glass	2.1 – 2.2 g/cm ³	
c_g	Heat capacity	0.8 – 1.6 J/g/K	
α	Thermal diffusivity	2.7×10^{-7} m ² /s	

In our case, laser source moves continuously in the direction transverse to the propagation one. As a result, laser beam passes the focal volume with lateral diameter $d_f = 2R_f$ during the heating time $t_h = d_f/V_s$ by applying $N = \nu \frac{2R}{V_s}$ laser pulses. Thus, the linear dependencies revealed in Fig. 3 can be presented as follows

$$\Lambda(N) = \xi N = \xi N_0 + \xi(N - N_0) = d_v + \xi N_1 \quad (7)$$

for the period of the void structure, and

$$E_a(N) = E_0 N = E_0 N_0 + E_0(N - N_0) = E_v + E_0 N_1 \quad (8)$$

for the threshold laser energy respectively, where N_0 is the minimum number of laser pulses per focusing spot in the decompaction regime; $N_1 = (N - N_0)$; d_v is the typical void diameter, and $E_v = E_0 N_0$ is the minimum laser energy per focusing spot required for decompaction. Thus, these dependencies indicate that only a small fraction of energy goes to the void formation. When the number of laser pulses overcomes N_0 , then a large fraction of energy is lost, and this amount rises linearly with the number of laser pulses as well as structure period.

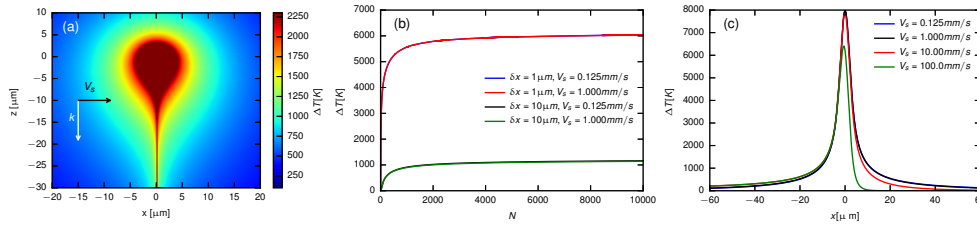


Fig. 5. (a) XZ view of base temperature distribution ($E_p = 2.2\mu J$, $V_s = 1\text{mm/s}$, $\nu = 500\text{kHz}$, $\omega_0 = 2.45\mu\text{m}$) after 10,000 pulses irradiated on the porous glass; (b) temporal profiles of base temperature increase in positions of $(1,0,0)\mu\text{m}$ and $(10,0,0)\mu\text{m}$ at various laser scanning speed; (c) 1D temperature increase along X axis at various scanning speed after 10,000 pulses illuminated on the material, as one can see, at speed lower than 10 mm/s the heat front propagates faster than the laser scan; Note, in this calculation, the coordinate is moving at speed of V_s ; for simplicity, heat parameters are set as constants with $c_g = 1.6\text{J/g/K}$, $\rho_g = 2.2\text{g/cm}^3$ and $\alpha = 2.7 \times 10^{-7}\text{m}^2/\text{s}$.

Material decompaction occurs when the absorbed energy is high enough to heat material in the focal region (at $d_f/2$) up to a temperature exceeding the glass softening temperature and when the energy source supplies enough energy for the void formation. It was estimated that $\approx 2.5\mu\text{J}$ per pulse is required for the tensile stress in the localized molten region of fused silica to exceed several MPa, which is enough for a void formation (see Ref. [9]). As one can see in Fig. 4(b), in our case $\approx 2.2\mu\text{J}$ is the laser energy per pulse, but at least E_v is required to create a void structure and this energy rises with N . The energy losses include energy spent for light reflection, scattering, and transmission. Additionally, laser energy is required for such effects as material ionization (both field and avalanche ionization processes), plasma heating, phase transitions (here, softening, densification, plasma formation), and it is also dissipated via pressure waves, heat conductivity, convection and viscous flow motion, and even radiation. As a result, only a very small fraction of the absorbed energy actually leads to the void formation.

Apparently, energy losses increase linearly with N , so that the most effective regime for void structure formation is when N is rather small, or at the highest laser writing speed required for the void structure formation (see Fig. 4(b)). In this case, voids are closely packed and $\Lambda = d_v$. The typical void size is $\approx 10\mu\text{m}$ corresponds to the radius of the molten and superheated region and exceeding the diameter of the focal region (around $4\mu\text{m}$), where gas/plasma phase is formed.

To estimate void size, we define the temperature required for void formation for the corresponding laser irradiation conditions by applying the Grady's criterion for spall in liquid [36]. According to the viscoelastic energy conservation law, the elastic energy of the deformation is defined as $\approx Y\sigma t^2$, where t is the deformation time limited by the time between two pulses $2\mu\text{s}$ and $\sigma = \frac{\Delta\rho}{\rho t}$ is the laser-induced strain rate, should be sufficient to do the work against the dissipation forces defined by $\eta\sigma$. The viscosity of porous glass is lower than that of the pristine fused silica and its dependencies on the glass porosity have been previously reported [37, 38]. For instance, for porosity of 26%, the viscosity is approximately ten times lower than it for the pristine silica. This way, it is possible to derive the maximum viscosity required for cavitation as follows $\eta_{max} = Y\sigma t^2 \approx 10^6\text{Pa} \cdot \text{s}$. These viscosities correspond to the temperature T_d of order 2500K, exceeding boiling temperature of the material. The results of the performed calculations presented in Fig. 5 indicate that the thermo-affected zone with the temperatures exceeding 2500K is around $10\mu\text{m}$, which agrees well with the experimental results (Fig. 3).

We note that for the solid material, another equation [18, 23] can be derived based on the energy conservation law as follows: assuming that the internal energy of the material with volume of $\frac{4}{3}\pi r^3$ is around the absorbed laser pulse energy, one gets $\frac{4}{3}\pi Y r_0^3 \approx E_{abs}$. The fact that voids grow

only slightly with laser energy means that upon a certain laser energy above the densification threshold, the absorbed fraction is almost constant, whereas energy losses should grow linearly. Then, for the diameter of a spherical void can be estimated as follows $d = C\sqrt[3]{\frac{6\alpha E_p}{\pi Y}}$, where α is the fraction of laser energy E_p absorbed by the material; Y is Young modulus; $C = \sqrt[3]{\frac{\Delta\rho}{\rho}}$ is the compression ratio. For fused silica, Young modulus $Y = 74.5\text{GPa}$, whereas for porous glass it can be smaller, for instance $Y = 17.5\text{GPa}$ was reported by Cerkauskaite et al. [23]. For the absorbed energy on the order of $2\mu\text{J}$, the estimation gives void diameter $\approx 10\mu\text{m}$, which is more than twice larger than the focusing diameter d_f .

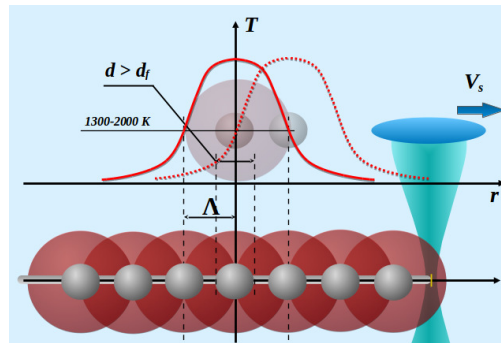


Fig. 6. Schematics illustrating the void structure formation

It remains to explain structure periodicity, and, namely, the observed almost linear period dependency on the number of laser pulses per focusing spot. Considering that cooling time is rather long and a scanning heating source supplies energy all the time, a stationary regime is expected in the absence of the void formation. In this regime, once void is formed, the temperature field outside the void is induced by two heat sources: (i) a moving laser source; and (ii) a static spherical heat source formed at the location of the previously formed void (Fig. 6). The solution of a static thermodynamic problem is straightforward and gives $T = Q/4\pi kr$ outside of the void, where k is thermal conductivity and Q can be considered to be proportional to E_0N , indicated by the revealed linear dependency of the decompaction threshold. Heat diffusion induces densification and softening. The fronts of these phase transitions propagate longer distances when more energy is absorbed, therefore $\Lambda = r_d = Q/4\pi kT_d$. Once laser overcomes the modified region, again enough energy can be spent for the next void. When r_d is smaller than $r_f/2$, we get a closely packed void structure, otherwise the voids are spaced with a distance Λ that rises linearly with N .

3. Conclusion

In conclusion, we have demonstrated that periodic void structures can be produced in a well-controlled manner inside porous glasses by femtosecond laser pulses. Particularly, we have demonstrated that trains of ultrashort laser pulses with a properly chosen energy per pulse and writing speed not only provide the required energy deposition, but also allow an efficient inscription of the periodic arrays of voids in these materials. Contrary to powerful single laser pulses that are known to produce explosion-like effects, pulse trains can be used to considerably reduce non-desirable effects, such as material cracking.

Both the obtained experimental results and the performed thermodynamic analysis have shown that the possibility of an efficient control over laser micromachining in volume relies on a better understanding of the physical mechanisms involved. For the given pulse repetition rate, the main

controlling parameters being the laser scanning speed and the mean energy per pulse, while the former defines both the structure period and the required laser energy per focusing spot. The period has been found to depend on the size of the densified region induced by the created almost static spherical heat source located at the void position. The final structure is induced by a superposition of two energy sources: the moving laser and the created static heat source.

Additionally, the performed analysis has indicated that the void formation is more efficient when the minimum number of laser pulses per focusing spot corresponds to the writing speed as high as about 0.47mm/s . Under these conditions, a compact void structure has been written in the porous glass, so that the structure period is equal to the void diameter. For lower scanning speed, both threshold and period increase linearly as a result of the rising energy losses. The lost energy goes mostly for material heating and densification thus leading to a reduced absorption at the passages between the voids.

The performed study thus provides a way of a well-controlled laser inscription of void arrays in the bulk of porous materials. The obtained results can be useful for advancing not only a wide range of photonics applications, but also for many applications in micro-fluidics, biology and other fields.

Funding

Campus France PHC KOLMOGOROV FormaLas project.

Acknowledgments

This work was supported by the PHC KOLMOGOROV FormaLas project, operated via Campus France. H.M. acknowledges the support of French Ministry of Science and Education for his PhD Scholarship. T.E.I. is grateful to ITMO Professorship & Fellowship program.